CARBON letters

Original Articles
Carbon Letters Vol. 14, No. 4, 234-242 (2013)

Removal of deltamethrin insecticide over highly porous activated carbon prepared from pistachio nutshells

A. F. Hassan[1,*], A. M. Youssef[2] and P. Priecel[3]

[1]Chemistry Department, Faculty of Science, Damanhour University, El-Gomhoria Street, 22511 Damanhour, Egypt
[2]Chemistry Department, Faculty of Science, Mansoura University, El-Gomhoria Street, 35516 Mansoura, Egypt
[3]Department of Physical Chemistry, Faculty of Chemical Technology, University of Pardubice, Studentska 573, 53210 Pardubice, Czech Republic

Article Info

Received 28 July 2013
Accepted 3 September 2013

***Corresponding Author**
E-mail: Asmz68@yahoo.com

Open Access

DOI: http://dx.doi.org/10.5714/CL.2013.14.4.234

This is an Open Access article distributed under the terms of the Creative Commons Attribution Non-Commercial License (http://creativecommons.org/licenses/by-nc/3.0/) which permits unrestricted non-commercial use, distribution, and reproduction in any medium, provided the original work is properly cited.

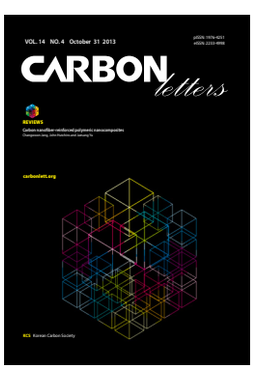

http://carbonlett.org

pISSN: 1976-4251
eISSN: 2233-4998

Copyright © Korean Carbon Society

Abstract

Potassium hydroxide-activated carbons (CK21, CK11, and CK12) were prepared from pistachio nutshells. Physicochemical properties of activated carbons were characterized by TGA, pH_{pzc}, Fourier transform infrared spectroscopy, scanning electron microscopy, and N_2-adsorption at -196°C. The examinations showed that activated carbons have high surface area ranging between 695-1218 m^2/g, total pore volume ranging between 0.527-0.772 mL/g, and a pore radius around 1.4 nm. The presence of acidic and basic surface C-O groups was confirmed. Batch adsorption experiments were carried out to study the effects of adsorbent dosage, temperature, initial concentration of adsorbate, and contact time on deltamethrin adsorption by activated carbons. The kinetic studies showed that the adsorption data followed a pseudo-second order kinetic model. The Langmuir model showed a maximum adsorption capacity of 162.6 mg/g at 35°C on CK12. Thermodynamic studies indicated that adsorption was spontaneous and increased with temperature, suggesting an endothermic process.

Key words: activated carbon, pistachio nutshells, insecticide, deltamethrin, adsorption

1. Introduction

Pesticides are considered one of the most hazardous groups of pollutants in water and air due to their high stability and toxicity, usage in huge quantities, and wide applications for many purposes, particularly the production of massive quantities of crops. In general, pesticides are defined as a diverse group or mixture of chemical compounds, biological agents, antimicrobials, disinfectants or devices that are intentionally applied for selective administration and attenuation against any pests including insects, plant pathogens, weeds, birds, nematodes, and microbes that detrimentally affect the production, processing, storage, transport, or marketing of food or agricultural compounds or are responsible for the destruction of property or spread of diseases [1-3]. The herbicide component bentazone was studied via adsorption removal over activated carbon cloth as an electrode and it was found that a change of pH from 2 to 7 reduced the adsorption capacity from 127 mg/g to 80 mg/g [4]. Deltamethrin is a synthetic pyrethroid insecticide that kills insects on contact and through digestion. It is used for many crops throughout the year, and consequently is widespread in the environment. Furthermore, it is non-degradable during storage for 6 months at 40°C, it is stable when exposed to atmospheric oxygen, and isomerization occurs upon exposure to sunlight. Acute effects on the human body include the following: ataxia, convulsions leading to muscle fibrillation and paralysis, diarrhea, edema, dermatitis, dyspnea, headache, irritability, hepatic microsomal enzyme induction, peripheral vascular collapse, rhinorrhea, serum alkaline phosphate elevation, tinnitus, vomiting, and death due to respiratory failure. Allergic reactions include the following manifestations: anaphylaxis, bronchospasm, eosinophil-

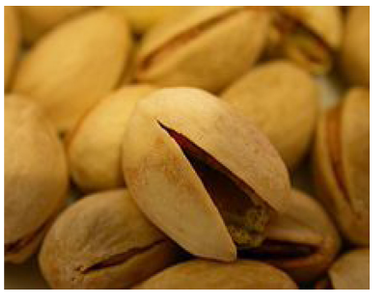

Fig. 1. Pistachio nutshells.

Table 1. Top 5 pistachio producing countries (Food and Agricultural Organization website)

Country	Iran	USA	Turkey	Syria	China
Production (Mt)	192 269	126 100	120 113	52 600	40 000

ia, fever, hypersensitivity pneumonia, sweating, pallor, pollinosis, sudden swelling of the face, eyelids, lips, and mucous membranes, and tachycardia. Chronic exposure effects in humans include choreoathetosis, hypotension, prenatal damage, and shock [5].

Adsorption on a solid surface is still the most important and useful method for removal of pollutants due to their high adsorption capacity, simple recovery process from the solid surface, and simple handling. Activated carbons are still the primarily used solid adsorbents due to their chemical inertness, high surface area, microporosity, presence of surface functional groups, renewability, capacity for simple surface modification to adsorb certain contaminants, and the possibility of production from solid agricultural waste byproducts. Activated carbons have the ability to adsorb various substances both from gas and liquid phases [6,7]. Activated carbons are produced from a solid carbonaceous material that is rich in carbon but low in inorganic content. Pistachio nutshells (Fig. 1) are considered one of the most useful and abundant renewable agricultural wastes, as reported by the Food and Agricultural Organization of the United Nations (Table 1).

The main objective of this research is to prepare potassium hydroxide (KOH)-activated carbons from pistachio nutshells. The following methods were used to characterize the prepared activated carbons: nitrogen adsorption at -196°C, scanning electron microscopy, thermogravimetric analysis, Fourier transform infrared spectroscopy (FT-IR) analysis of the surface chemistry, pH_{pzc}, surface pH analysis, and measurement of deltamethrin adsorption capacity at different temperatures. Special attention was paid to kinetic and thermodynamic studies.

2. Materials and Methods

2.1. Materials

2.1.1. Adsorbents

Pistachio nutshells collected from pistachio nuts obtained from El-Mansoura City (Egypt) local markets were used as a precursor. They were washed with distilled water to remove any adherent impurities and then dried at 110°C for 24 h and then ground and sieved to yield particle size ranging from 1-2 mm. Three activated carbon samples were prepared via a two-step method: carbonization of the dried precursor at 600°C in the absence of air using a stainless steel reactor (600 mm × 40 mm) at a rate of 10°C/min. up to 600°C. The carbonized sample was cooled and soaked with a certain weight of KOH in 50 mL of distilled water for 48 h at room temperature, followed by drying at 110°C and finally activated at 750°C for 4 h. Three samples were prepared using different carbonized samples: KOH ratios. These samples were designated as CK21, CK11, and CK12, where the ratio of carbonized samples to KOH weights was 2:1, 1:1, and 1:2, respectively. Prepared samples were washed several times with distilled water and then dried at 110°C to reach a constant weight, and then stored in clean and dry-fitted glass bottles.

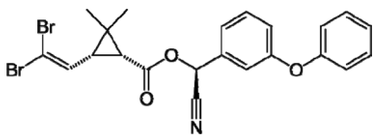

Fig. 2. Chemical structure of deltamethrin.

2.1.2. Adsorbate

Deltamethrin insecticide was provided by KZ Company for Pesticides and Chemical Industries (Kafr El-Ziat City-Egypt) in 98% purity and a molar mass of 505.21 g/mol with a chemical structure as shown in Fig. 2. The solubility of deltamethrin in water is low, and a mixed solvent of ethanol/water (50 vol/vol% ratio) was therefore used to allow preparation of the required experimental concentrations.

2.2. Techniques

2.2.1. Surface chemistry of samples

To obtain a complete picture of the samples surface chemistry was determined using the following technique: FT-IR using a Mattson 5000 FT-IR spectrometer in a range between 4000 and 400 cm^{-1}, where discs were prepared by mixing 1 mg of dried carbon sample with 500 mg of KBr (spectroscopic purity, Merck) in an agate mortar followed by pressing the mixture at 5 ton/cm^3 for 3 min and 10 ton/cm^3 for 5 min under vacuum. The pH of the supernatant was determined by shaking 0.5 g of the carbon sample with 25 mL of CO_2-free distilled water for 24 h; the pH of the supernatant was then measured. pH_{pzc} (point of zero charge) was determined by adding 50 mL of sodium chloride into several closed flasks. The pH within each flask was adjusted to values ranging from 2 to 12 by adding either sodium hydroxide (0.1 M) or hydrochloric acid (0.1 M).Then, 0.2 g of carbon was added to each flask, the flasks were shaken for 48 h, and the final pH was measured. The pH_{pzc} is defined as the point where the curve of pH_{final} vs. $pH_{initial}$ crosses the line pH_{final}= $pH_{initial}$ [8].

2.2.2. Thermal gravimetric analysis and weight loss during drying

Thermal gravimetric analysis (TGA) were performed to identify the thermal behavior of pistachio nutshells as a raw material and CK12 as a selected activated sample using a differential thermal analyzer (Shimadzu DTA-50, Japan). The weight loss during drying was determined for the raw material and activated sample by

weighting 0.5 g of the sample and heating for 24 h in an oven at 110°C until the weight of the sample became constant.

2.2.3. Textural characterization

Textural characterization was performed using nitrogen adsorption at -196°C to evaluate the specific surface area, pore radius, and total pore volume for the investigated activated carbon using a Quantachrome NOVA2000 gas sorption analyzer.

2.2.4. Scanning electron microscopy

Scanning electron micrographs (SEM) of CK12 were obtained using a JEOL 6400. Prior to the measurement, the samples were dried at 110°C for 4 h. A thin layer of gold was coated on each sample for charge dissipation.

2.3. Batch equilibrium studies

Adsorption isotherms were obtained from solutions of deltamethrin with different initial concentrations and an equal mass of activated carbons placed in a set of Erlenmeyer flasks (100 mL) at two different temperatures (19°C and 35°C) that were placed in an isothermal shaker (19°C or 35°C) for 24 h to reach equilibrium as a solid-solution mixture. The flasks were then removed from the shaker and the final concentration of deltamethrin in the supernatant was measured at 282 nm using a UV-vis spectrophotometer Unicam UV/VIS 5625. The adsorbed amount q_e (mg/g) was calculated as follows:

$$q_e = \frac{(C_o - C_e)}{W}, \quad (1)$$

where C_o and C_e (mg/L) are the concentrations of deltamethrin at the beginning and at equilibrium, respectively, V is the volume of solution (L), and W is the mass (g) of dry activated carbons.

2.4. Effects of dosage

Effects of dosage were checked in a set of Erlenmeyer's flasks containing the same volume and the same concentrations of deltamethrin and mixed with different weights of activated carbons, shaken at a specified temperature for 24 h until equilibrium was reached. After this procedure the residual concentration of deltamethrin was determined.

2.5. Batch kinetic studies

The kinetic study procedures were identical to those of the equilibrium experiments. The solutions of the samples were taken at present time intervals, and the concentrations of insecticide were similarly measured.

3. Results and Discussion

3.1. Characterization of precursor and activated carbons

3.1.1. Solid density, drying weight loss, ash content, and thermogravimetry

Impregnation of a carbonized (non-activated carbons) sample in a concentrated KOH solution for a long time was followed by drying and activation at 750°C. Drastic changes in the texture and porous surface development were anticipated when KOH reacted with carbon atoms, which results in a loss of carbon content and an increase in the percent of ash content according to the following equation:

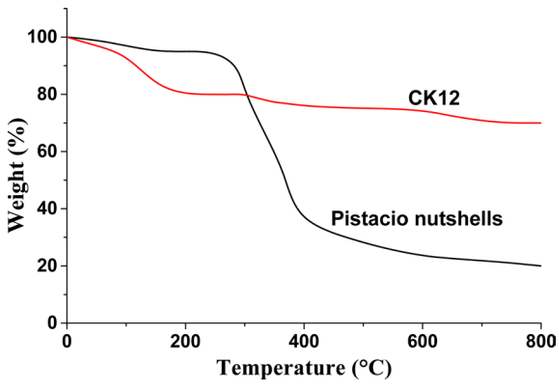

Fig. 3. TGA profile of pistachio nutshells and CK12 activated carbon.

$$4KOH + C \rightarrow K_2O + K_2CO_3 + 2H_2 \quad (2)$$

Some reactions may take place due to decomposition of KOH, as listed below:

$$2\ KOH \rightarrow K_2O + H_2O \quad (3)$$
$$C + H_2O \rightarrow H_2 + CO \quad (4)$$
$$CO + H_2O \rightarrow H_2 + CO_2 \quad (5)$$
$$K_2O + CO_2 \rightarrow K_2CO_3 \quad (6)$$
$$K_2O + H_2 \rightarrow 2\ K + H_2O \quad (7)$$
$$K_2O + C \rightarrow 2\ K + CO \quad (8)$$
$$K_2CO_3 + 2C \rightarrow 2K + 3CO \quad (9)$$

It was reported that the decomposition of KOH, the reduction of the carbon framework, the evolution of hydrogen in reaction Eq. (2), and the evolution of carbon dioxide and steam as oxidizing gases in other reactions could be responsible for the production of new pores and could also lead to the erosion of pore walls [9]. Table 2 indicates that 1) the solid density for pistachio nutshells is lower than the solid density of activated samples and increases with an increase in ratio of KOH to carbonized sample; 2) weight loss during drying increases with the activation by KOH, where weight loss during drying for CK12 is about 3.8 times higher than that of pistachio nutshells. This is a logical result of the higher surface area and production of carbon-oxygen functional groups on the activated samples, which enhance the surface adsorption of water molecules; 3) ash content for pistachio nutshells is very low (1.01%) due to the higher amount of cellulose and lignin [10]; and 4) during activation, KOH reduces the carbon content in the samples followed by an increase in ash content, which intensifies with an increase of the KOH ratio.

The shape of the TGA profile depends on the thermal behavior of the biomass, which is related to the chemical composition and chemical bonding in the material structure. TGA provide provides an indication of the carbon content in the precursor and can serve as primary data for the production of activated carbon. Fig. 3 shows

Table 2. Solid density, weight loss upon drying, ash content, pH of supernatant, and pH_{pzc} for precursor and investigated samples

Sample	Solid density (g/cm^3)	Weight loss on drying (%)	Ash content (%)	pH (supernatant)	pH_{pzc}
Pistachio nutshells	1.30	2.90	1.01	6.50	6.40
CK21	1.50	6.51	3.20	7.70	7.50
CK11	1.61	8.62	4.51	7.81	7.61
CK12	1.68	10.80	5.81	8.00	7.80

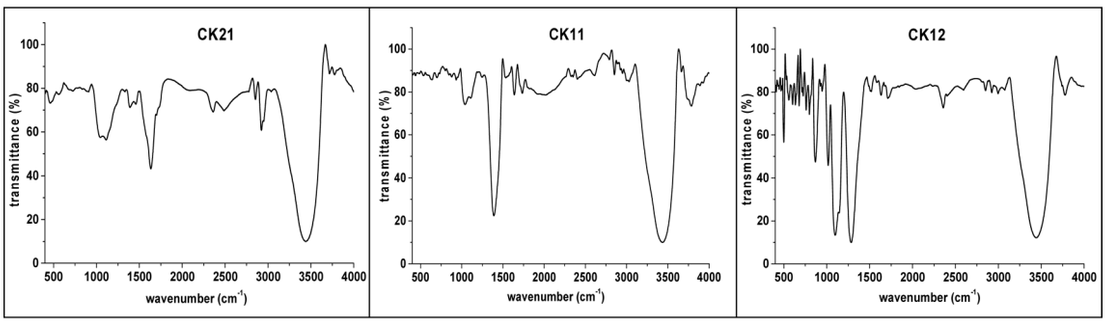

Fig. 4. FTIR spectra of the investigated activated carbons.

the effect of temperature on the residual weight of the raw pistachio nutshells and CK12 as a selected activated carbon sample. The TGA profile of pistachio nutshells shows that weight loss under 150°C corresponds to moisture content in the pistachio nutshells and was found to be around 3 wt%. Carbonization reactions started to dominate beyond 150°C. It is known that degradation of hemicelluloses starts at 200-260°C and cellulose degradation occurs at around 240-350°C. Lignin is more stable than cellulose and hemicelluloses, and decomposes at a temperature range of 280-800°C [11]. The minor extractives of inorganic constituents and their catalytic effects also influence the weight loss of biomass during pyrolysis [12]. Significant weight loss was observed between 275°C and 520°C, and is due to decomposition of the main components of the pistachio nutshells and removal of the gaseous volatile matter from the structure. At ~750°C degradation of the lignocellulosic structure was nearly completed. Carbonization at 600°C was selected to obtain carbonized samples from pistachio nutshells. The activated carbon sample (CK12) was not strongly affected by temperature, where the decrease in weight under 150°C may be related to the removal of adsorbed moisture. This effect was more pronounced in CK12 than in pistachio nutshells due to the higher surface area of the former and the presence of hydrophilic C-O functional groups, which enhance moisture adsorption onto CK12.

3.1.2. pH of supernatant, pH_{pzc}, and FT-IR

Surface chemistry of a solid adsorbent is a very important factor in the determination of the adsorption capacity and selectivity and in identifying the chemical nature of the activated carbon surface. The values of the supernatant pH and the values of pH_{pzc} are summarized in Table 2. The supernatant pH and pH_{pzc} of the precursor are comparable. The supernatant pH and pH_{pzc} of the KOH-activated carbons are also comparable and increase with an increase of the amount of KOH used during activation.

FT-IR is mainly used as a qualitative technique for the study of surface chemical functional groups on activated carbons. Carbons are black solid materials that absorb almost all radiation in a range of 360-800 nm and the peaks obtained in FT-IR are commonly a sum of the interactions of the different types of surface groups [13]. Fig. 4 shows the FT-IR spectra of KOH-activated samples. The bands located at around 3500 cm^{-1} can be assigned to the –OH stretching vibration mode of hydroxyl functional groups [14].The peak at around 2929 cm^{-1}, which is easily observed in the case of CK21, indicates the presence of a methylene group (–CH2–) with CH stretching [15]. The peak at around 1745 cm^{-1} with observable transmittance in the case of CK21 and almost absent in the cases of CK11 and CK12 is attributed to lactone groups. The bands located at around 1380 and 1465 cm^{-1}are due to δ(C-H) vibrational bands for $–CH_3$ and –CH2– groups, respectively. Bands in the range of 1000-1300 cm^{-1} can be attributed to vibrations of various C-O bonds, such as those in ethers, phenols, and esters [16,17]. The bands in the region of 850-440 cm^{-1} are ascribed to alkenes vibrations. Generally, the surface oxides on carbon can exhibit acidic as well as basic properties. The acidic surface properties are caused by the presence of carboxyl groups, lactones or lactols (Fig. 5a), and hydroxyl groups of a phenolic character [18]. Basic groups are usually structures corresponding to chromene- or pyrone-like structures [19] (Fig. 5b).

3.1.3. Textural characterization of activated carbons

Adsorption efficiency of activated carbon depends mainly on its porous structures and its surface functional groups. Many experiments have been established to determine specific surface area, total pore volume, pore radius or pore size distribution. A nitrogen adsorption process at -196°C is still the primary method in textural characterization of porous materials, especially activated carbons. Fig. 6 shows the adsorption isotherms for CK21, CK11, and CK12, which are type I in their initial stage but show

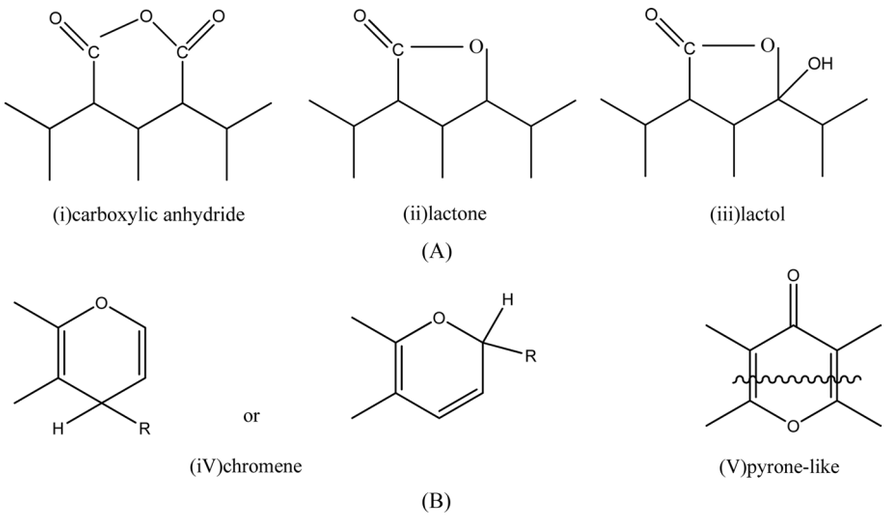

Fig. 5. Acidic surface groups (A) and basic surface groups (B).

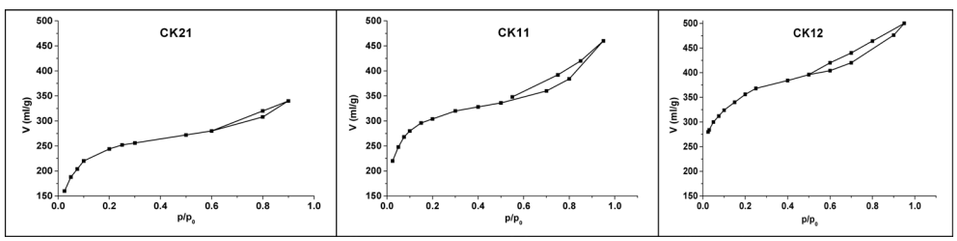

Fig. 6. Nitrogen adsorption isotherms at -196°C for the investigated activated carbons.

some characteristics of type IV in later stages. The observation of a hysteresis loop indicates the presence of wider pores, which may be related to the corrosive effect of KOH on the microporous carbon walls. The values of surface area (m^2/g), total pore volume (mL/g), and pore radius (nm) are summarized in Table 3. The linear Brunauer-Emmett-Teller (BET) plots enabled us to determine the surface area for different activated samples (S_{BET} [m^2/g]) and therefore to calculate the mean pore radius $\bar{r}$(nm) according to the following equation:

$$\bar{r}(nm) = \frac{2V_T(mL/g)}{S_{BET}(m^2/g)} x10^3 \quad (10)$$

where V_T is the adsorbed volume near the saturation point, i.e.at $p/p^o \approx 0.95$, multiplied by the factor 15.5×10^{-4}. Table 3 reveals that 1) the specific surface areas for the KOH-activated samples increase in the order 695 < 956 < 1218 m^2/g with change in the ratio of weight of the carbonized sample to KOH weight in the order 2:1 < 1:1 < 1:2, respectively, indicating that as the amount of potassium hydroxide activating agent increases the porosity and surface area also increase, but that the increase is not linear; 2) total pore volumes range between 0.527-0.772 mL/g, and increase with the amount of KOH, and it is not surprising that the effect of the activating agent is based mainly on the creation of new pores; and 3) pore radius measurements indicate a surface containing micropores that decrease in the order 1.520 > 1.48 > 1.27 nm for CK21, CK11, and CK12, respectively, thus demonstrating the capability of potassium hydroxide to create new pores rather than to widen existing pores.

Table 3. BET-Surface area, total pore volume, and pore radius for activated carbon samples

Sample	S_{BET} (m^2/g)	V_T (mL/g)	$\bar{r}$ (nm)
CK21	695	0.527	1.52
CK11	956	0.708	1.48
CK12	1218	0.772	1.27

BET: Brunauer-Emmett-Teller.

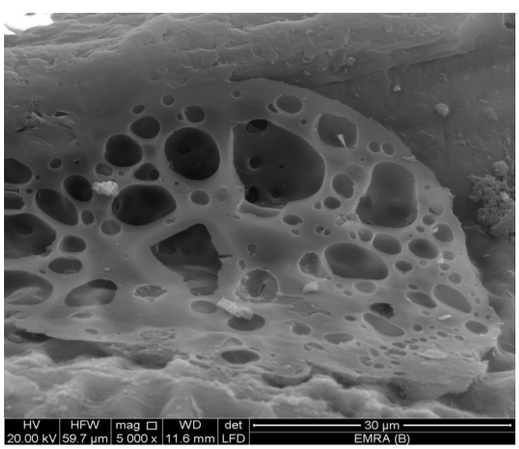

Fig. 7. SEM image of CK12 sample.

The SEM micrograph obtained at a magnification of 5000× clearly indicates the porous structure of the activated carbons (Fig. 7). It shows that KOH-activated carbons exhibit a wide range of pore radiuses and lack a definite morphology, possibly due to carbonization at 600°C and activation with KOH at750°C.

3.2. Adsorption of deltamethrin

3.2.1. Effect of adsorbent dosage

An experiment was carried out to study the effect of adsorbent dosage on deltamethrin adsorption. Various quantities of CK12, selected as an activated carbon sample, were contacted with a fixed initial pesticide concentration. Uptake of pesticide after a contact time of 24 h versus the adsorbent dosage (g/L) is shown in Fig. 8. The results indicate that the pesticide uptake increased from 67 to 93% when the CK12 dose was increased from 0.5 to 7.5 g/L, respectively. The maximum uptake of deltamethrin was thus obtained at a higher adsorbent dosage. This is due to the greater availability of adsorption sites for the adsorbate as the adsorbent dosage is increased, thus enhancing the deltamethrin uptake [20]. Also, with increasing adsorbent loading, the quantity of deltamethrin adsorbed onto the unit weight of the adsorbent is reduced, thus causing a decrease in the q_e (mg/g) values with increasing activated carbon loading.

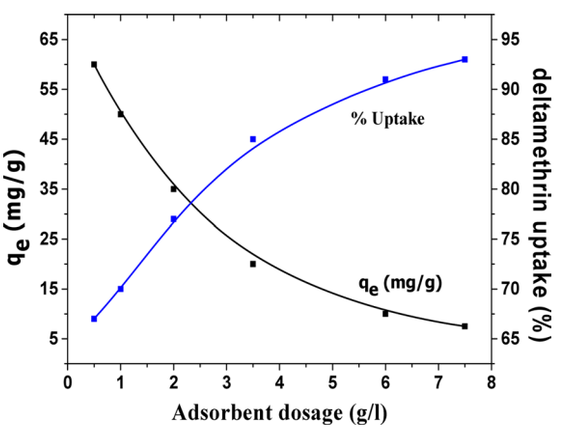

Fig. 8. Effect of adsorbent (CK12) dosage.

3.2.2. Adsorption kinetics

The effect of contact time was investigated to determine the equilibrium time for deltamethrin adsorption on CK21 and CK12. Fig. 9a shows an increase in deltamethrin removal for all initial concentrations of insecticide investigated. However, the adsorption was faster at the initial times but progressively slowed down with time until equilibrium was finally attained. This is attributed to the large number of vacant sites available for adsorption at the initial stages. The experimental data obtained from the adsorption of deltamethrin on CK21 and CK12 were fitted with a pseudo-second order (PSO) kinetic model but could not be fitted with a pseudo-first order kinetic model, possibly due to the dependence of the adsorption process on both the adsorption surface and deltamethrin itself. The linearized form of the PSO reaction equation can be written as:

$$\frac{t}{q_t} = \frac{1}{Kq_e^2} + \frac{1}{q_e}t \tag{11}$$

where K is the PSO rate constant (g/mg.min), t is the time in minutes, q_t is the amount adsorbed in time t (mg/g), and q_e is the equilibrium adsorbed amount (mg/g). The linearized plot for the PSO equation is shown in Fig. 9b. Table 4 contains the kinetically determined data for deltamethrin adsorption on CK21 and CK12 as selected activated samples. Upon inspection of the data shown in Table 4, we can observe that the q_e values are 163 and 177 mg/g for CK21 and CK12, respectively. Column 3 of Table 4 displays the PSO rate constant, which is 1.850×10^{-4} and 2.363×10^{-4} g/mg.min for CK21 and CK12, respectively. Correlation coefficient (R^2) values are presented in Table 4, which approached unity and indicate the applicability of the PSO kinetic model for deltamethrin adsorption on KOH-activated samples.

The intraparticle diffusion model was first proposed by Weber and Morris [21], who concluded that the uptake is proportional to the square root of the contact time during the adsorption, i.e.,

$$q_t = k_d t^{0.5} + C \tag{12}$$

where k_d is the rate constant of the intraparticle transport (mg/g. min). The value of k_d was obtained from the slope of a straight line where C is the intercept. According to the Weber and Morris model, multilinearity may be obtained when q_t is plotted versus $t^{0.5}$, as shown in Fig. 10. This indicates two steps are involved in the present investigation. The first sharper line indicates the external surface adsorption. The second portion is gradual adsorption, referring to

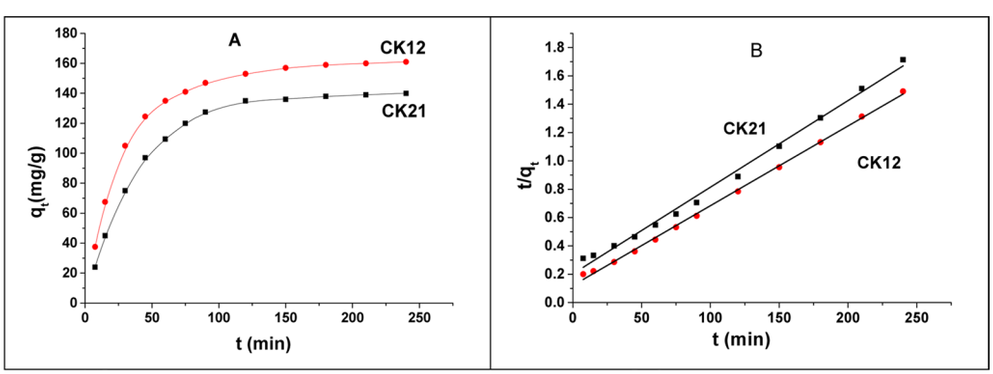

Fig. 9. Kinetic adsorption curves (A) and pseudo-second order kinetic plots (B) for adsorption of deltamethrin on CK21 and CK12.

Table 4. Kinetic studies for adsorption of deltamethrin on CK21 and CK12

Samples	PSO plot			Morris-Webber plot	
	q_e (mg/g)	K (g/mg.min)	R^2	k_d (mg/g.min)	R^2
CK21	163	1.850 × 10-4	0.99342	17.4157	0.99437
CK12	177	2.363 × 10-4	0.99841	19.7480	0.96891

PSO: pseudo-second order.

the intraparticle diffusion controlled adsorption process. If the lines do not pass through the origin, the intraparticle diffusion is not the rate limiting step and this indicates the effect of film diffusion on the adsorption of deltamethrin [8]. Table 4 presents the values of the constants k_d and C, as calculated by the Weber and Morris model.

3.2.3. Equilibrium adsorption isotherms

The adsorption isotherm indicates how the adsorbed molecules are distributed between the solid surface phase and the liquid phase when the adsorption process reaches an equilibrium state. Several adsorption models have been reported in the literature to describe the adsorption data of isotherms. The amount of deltamethrin adsorbed, q_e (mg/g), is plotted against the equilibrium concentration C_e (mg/L), as shown in Fig. 11. The isotherms have been classified according to the Giles classification into four main groups, L, S, H, and C [22]. According to the above classification the three KOH-activated carbons show L-type isotherms. The Langmuir and Freundlich are the most frequently used models. In this work the Langmuir model was used to describe the relation between the amounts of deltamethrin adsorbed, C_e/q_e, and the equilibrium concentration C_e (mg/L). Langmuir's isotherm model postulates that adsorption occurs on a homogenous surface by monolayer adsorption without interaction between adsorbed molecules, with uniform energies of adsorption on the surface, and no transmigration of adsorbate molecules on the solid surface plane. The linear form of the Langmuir isotherm equation is represented by the following equation [23]:

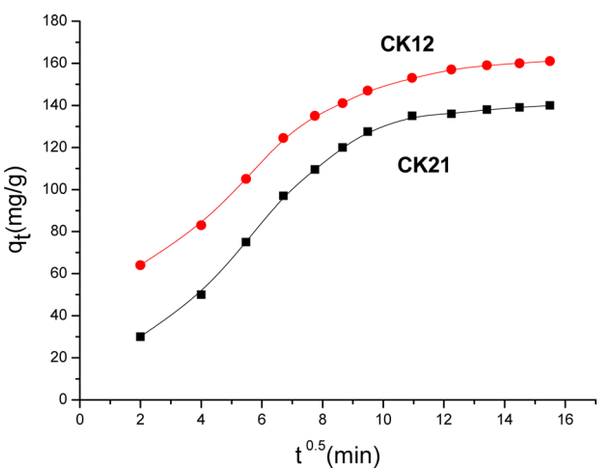

Fig. 10. Representative intraparticle diffusion plots for deltamethrin adsorption on CK21 and CK12.

$$\frac{C_e}{q_e} = \frac{1}{bq_m} + \frac{C_e}{q_m} \quad (13)$$

where q_e is the amount adsorbed at equilibrium time (mg/g), C_e is the equilibrium concentration of deltamethrin (mg/L), q_m is the maximum adsorption capacity (mg/g), and b is known as the Langmuir constant (L/mg) and it is related to the heat of adsorption. The plot of C_e/q_e versus C_e of deltamethrin on activated carbons (CK21, CK11, and CK12) will give a straight line with slope = $1/q_m$ and an intercept = $1/bq_m$, as shown in Fig. 12. Applying the Langmuir model at two different temperatures, 19°C and 35°C, enables us to calculate the maximum adsorption capacity (mg/g) and the Langmuir constant (L/mg) at every temperature with a higher correlation coefficient (R^2), which ranged between 0.99413 and 0.99948, indicating a good linear fit for Langmuir's model. From the results shown in Table 5 we can conclude that at constant temperature q_m increases in the order CK21 < CK11 < CK12 due to the increase in specific surface area and total pore volume (Table 3), which introduces more available pores for adsorption of deltamethrin. Carrying out the adsorption at 35°C, we observed a significant increase in deltamethrin adsorption, which may be discussed on the basis of the endothermic nature of all the adsorption processes involving intraparticle diffusion, boundary

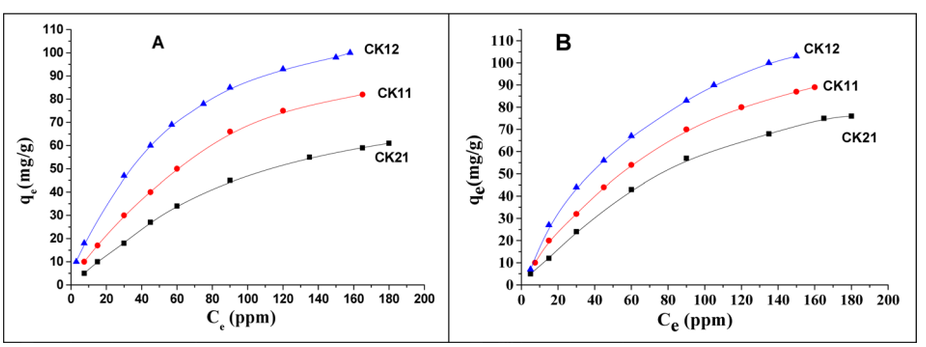

Fig. 11. Adsorption isotherms of deltamethrin for CK21, CK11, and CK12 at 19 °C (A) and 35 °C (B).

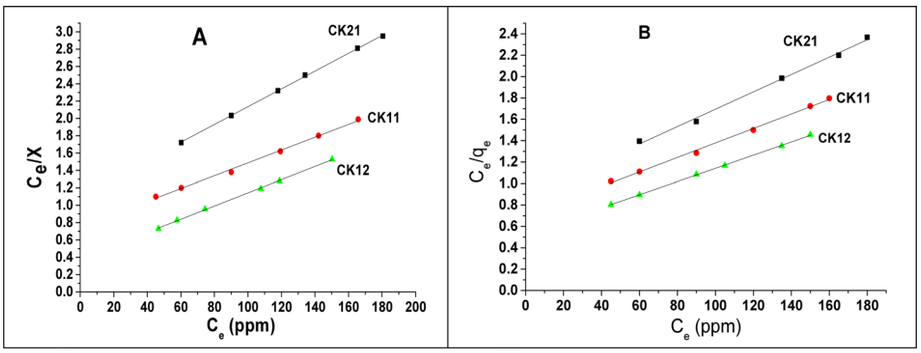

Fig. 12. Linearized form of Langmuir equation for deltamethrin adsorption on CK21, CK11, and CK12 at 19 °C (A) and 35 °C (B).

Table 5. Langmuir isotherm constants for deltamethrin adsorption on CK21, CK11, and CK12 at 19°C and 35°C

Sample	19°C			35°C		
	R^2	q_m (mg/g)	b (L/mg)	R^2	q_m (mg/g)	b (L/mg)
CK21	0.99948	97.3	0.01927	0.99413	123	0.12449
CK11	0.99605	130.2	0.02988	0.99675	147	0.24787
CK12	0.99909	135.9	0.12827	0.99942	162.6	0.68617

Table 6. Thermodynamic parameters for deltamethrin adsorption on CK21, CK11, and CK12 at 19°C and 35°C

Sample	19°C			35°C		
	K^O	ΔG^o (kJ/mol)	ΔS^o (kJ/mol.K)	K^O	ΔG^o (kJ/mol)	ΔS^o (kJ/mol.K)
CK21	5.233	-4.018	0.3124	5.912	-4.550	0.2979
CK11	5.428	-4.107	0.3528	6.423	-4.763	0.3366
CK12	6.018	-4.357	0.2852	6.809	-4.912	0.2722

layer diffusion, and surface adsorption processes. Also, raising the temperature may increase the kinetic energy of deltamethrin molecules and enhance the rate of diffusion of the adsorbate [20].

3.2.4.Thermodynamic parameters of deltamethrin adsorption

Thermodynamic parameters of deltamethrin adsorption on CK21, CK11, and CK12 were determined at 19 and 35°C. Thermodynamic parameters (Table 6), namely the thermodynamic equilibrium constant K_o, Gibbs free energy (ΔG^o), enthalpy change (ΔH^o), and entropy change (ΔS^o), were calculated using the following equations:

$$K_o = C_s/C_e \quad (14)$$

where C_s is the surface concentration of deltamethrin and C_e the equilibrium concentration.

$$\Delta G^o = -RT \ln K_o \quad (15)$$

where R is the universal gas constant (8.314×10^{-3} kJ.K^{-1}.mol^{-1}).

$$\Delta H^o = R\left(\frac{T_1 T_2}{T_2 - T_1}\right) 2.303 \log \frac{b_2}{b_1} \quad (16)$$

where b_1 and b_2 are the Langmuir constants at 19 and 35 °C, respectively.

$$\Delta S^o = \frac{\Delta H^o - \Delta G^o}{T} \quad (17)$$

The values of K_o increased with an increasing ratio of KOH: carbon, indicating an increase in the adsorption capacity, which could be related to an increase in the specific surface area and total pore volume of activated carbons. Based on the values of the obtained thermodynamic parameters (Table 6), the negative values of ΔG^o indicate spontaneous adsorption of deltamethrin on the activated carbon samples. Adsorption of deltamethrin can be considered as physisorption when the change in free energy for this process ranges between -4.018 and -4.912 kJ.mol^{-1}, because it is known that the absolute magnitude of the change in free energy for physisorption is between -20 and 0 kJ.mol^{-1}and that chemisorption occurs between -80 and -400 kJ.mol^{-1} [24]. It should also be noted that the change in free energy decreases with an increase in temperature, which indicates an increase in adsorption capacity with a rise in temperature. The positive values of entropy change reflect the increased randomness at the solid/solution surface. This is a direct consequence of enhancement of the mobility and extent of penetration within activated carbon pores and overcoming the activation energy bar-

rier and enhancing the rate of intraparticle diffusion. The positive values of ΔH^o (around 88.3 kJ/mol) confirm the endothermic nature of adsorption and explain the increase in adsorption capacity of the investigated samples to deltamethrin with a temperature increase.

4. Conclusions

Potassium hydroxide activated carbons with high adsorption capacity for deltamethrin insecticide were prepared from pistachio nutshells. SEM and nitrogen adsorption at -196°C showed microporosity of activated carbons with a pore radius of around 1.4 nm. FT-IR and pH_{pzc} indicated the presence of acidic and basic functional groups. The kinetic studies demonstrated that adsorption of deltamethrin on KOH-activated carbons is a PSO reaction. The adsorption of deltamethrin is very rapid in the initial stage and slowed down while approaching equilibrium, indicating that intraparticle diffusion is not the only rate controlling step in the adsorption process. Thermodynamic studies indicated an endothermic and spontaneous nature for adsorption of deltamethrin on activated carbons.

References

[1] Corsini E, Liesivuori J, Vergieva T, Van Loveren H, Colosio C. Effects of pesticide exposure on the human immune system. Hum Exp Toxicol, **27**, 671 (2008). http://dx.doi.org/10.1177/ 0960327108094509.

[2] Daneshvar N, Aber S, Khani A, Khataee AR. Study of imidaclopride removal from aqueous solution by adsorption onto granular activated carbon using an on-line spectrophotometric analysis system. J Hazard Mater, **144**, 47 (2007). http://dx.doi.org/10.1016/j.jhazmat.2006.09.081.

[3] Dich J, Zahm SH, Hanberg A, Adami HO. Pesticides and cancer. Cancer Causes Control, **8**, 420 (1997).

[4] Ania CO, Béguin F. Mechanism of adsorption and electrosorption of bentazone on activated carbon cloth in aqueous solutions. Water Res, **41**, 3372 (2007). http://dx.doi.org/10.1016/j.watres.2007. 03.031.

[5] Hallenbeck WH, Cunningham KM. Pesticides and Human Health, Springer-Verlag, New York (1985).

[6] Youssef AM. Moisture sorption in relation to some characteristics of coal. Carbon, **12**, 433 (1974). http://dx.doi.org/10.1016/0008-6223(74)90009-8.

[7] Youssef AM, El-Shobaky GA, El-Nabarawy T. Adsorption properties of carbons in relation to the various methods of activation. Surf Technol, **7**, 451 (1978). http://dx.doi.org/10.1016/0376-4583(78)90023-7.

[8] Youssef AM, Ahmed AI, El-Bana UA. Adsorption of cationic dye (MB) and anionic dye (AG 25) by physically and chemically activated carbons developed from rice husk. Carbon Lett, **13**, 61 (2012). http://dx.doi.org/10.5714/CL.2012.13.2.061.

[9] Guo Y, Yang S, Yu K, Zhao J, Wang Z, Xu H. The preparation and mechanism studies of rice husk based porous carbon. Mater Chem Phys, **74**, 320 (2002). http://dx.doi.org/10.1016/S0254-0584(01)00473-4.

[10] Yeganeh MM, Kaghazchi T, Soleimani M. Effect of raw materials on properties of activated carbons. Chem Eng Technol, **29**, 1247 (2006). http://dx.doi.org/10.1002/ceat.200500298.

[11] Özsin G. Production and characterization of activated carbon from pistachio-nut shell [MS Thesis], Middle East Technical University, Ankara, Turkey (2011).

[12] González JF, Román S, Encinar JM, Martínez G. Pyrolysis of various biomass residues and char utilization for the production of activated carbons. J Anal Appl Pyrolysis, **85**, 134 (2009). http://dx.doi.org/10.1016/j.jaap.2008.11.035.

[13] Matos J, Nahas C, Rojas L, Rosales M. Synthesis and characterization of activated carbon from sawdust of Algarroba wood. 1. Physical activation and pyrolysis. J Hazard Mater, **196**, 360 (2011). http://dx.doi.org/10.1016/j.jhazmat.2011.09.046.

[14] Aguilar C, García R, Soto-Garrido G, Arriagada R. Catalytic wet air oxidation of aqueous ammonia with activated carbon. Appl Catal B, **46**, 229 (2003). http://dx.doi.org/10.1016/S0926-3373(03)00229-7.

[15] Ahmad AL, Loh MM, Aziz JA. Preparation and characterization of activated carbon from oil palm wood and its evaluation on Methylene blue adsorption. Dyes Pigments, **75**, 263 (2007). http://dx.doi.org/10.1016/j.dyepig.2006.05.034.

[16] Liu QS, Zheng T, Wang P, Guo L. Preparation and characterization of activated carbon from bamboo by microwave-induced phosphoric acid activation. Ind Crops Prod, **31**, 233 (2010). ttp://dx.doi.org/10.1016/j.indcrop.2009.10.011.

[17] Yang T, Lua AC. Characteristics of activated carbons prepared from pistachio-nut shells by physical activation. J Colloid Interface Sci, **267**, 408 (2003). http://dx.doi.org/10.1016/S0021-9797(03)00689-1.

[18] Boehm HP. Surface oxides on carbon and their analysis: a critical assessment. Carbon, **40**, 145 (2002). http://dx.doi.org/10.1016/S0008-6223(01)00165-8.

[19] Jankowska H, Świątkowski A, Choma J, Kemp TJ. Active Carbon, E. Horwood, New York (1991).

[20] Aravindhan R, Fathima NN, Rao JR, Nair BU. Equilibrium and thermodynamic studies on the removal of basic black dye using calcium alginate beads. Colloids Surf A, **299**, 232 (2007). http://dx.doi.org/10.1016/j.colsurfa.2006.11.045.

[21] Weber W, Morris J. Kinetics of adsorption on carbon from solution. J Sanit Eng Div Am Soc Civ Eng, **89**, 31 (1963).

[22] Malik PK. Use of activated carbons prepared from sawdust and rice-husk for adsorption of acid dyes: a case study of Acid Yellow 36. Dyes Pigments, **56**, 239 (2003). http://dx.doi.org/10.1016/S0143-7208(02)00159-6.

[23] Langmuir I. The adsorption of gases on plane surfaces of glass, mica and platinum. J Am Chem Soc, **40**, 1361 (1918). http://dx.doi.org/10.1021/ja02242a004.

[24] Yu Y, Zhuang YY, Wang ZH. Adsorption of water-soluble dye onto functionalized resin. J Colloid Interface Sci, **242**, 288 (2001). http://dx.doi.org/10.1006/jcis.2001.7780.